Autofocus for SAR images in strongly asymmetrical bistatic configurations

Hubert Cantalloube, Jean-François Nouvel, Olivier Boisot

Autofocus for SAR images in strongly asymmetrical bistatic configurations

Hubert M.J. Cantalloube[a], Jean-François Nouvel[b], and Olivier Boisot[b]
[a]ONERA Université Paris Saclay, F-91123 Palaiseau, France
[b]ONERA École de l'Air, F-13661 Salon CEDEX AIR-France

Abstract

ONERA experimented bistatic satellite to aircraft SAR imaging with its lightweight SAR system BuSARd receiving TerraSAR transmitted signal at X-band with two channels for direct and terrain scattered paths. Static receiver experiment shown that the direct path signal is instrumental in clock synchronisation. Later, two flight experiments with anti-parallel and parallel paths were conducted showing that the trajectory error influences the focusing mainly through the clock synchronisation error from non-modeled direct path length. Significance of the receiving aircraft velocity was also emphasized from the anti-parallel acquisition.

1 Background for the experiment

ONERA has experimented bistatic aircraft to aircraft SAR imaging since 2003 with the E-SAR system of DLR along parallel trajectories, later (2009) between its heavy SAR system RAMSES and its lightweight BuSARd system along non parallel trajectories with different velocities, and eventually (2010) with the FOI LoraSAR system on varied time-varying configuration such as circle transmit to linear receive trajectories.
These three experiments emphasized the critical role of clock synchronisation between the transmitting and receiving radars for image focusing and image registration.
During the early ONERA/DLR and ONERA/ONERA experiment, the clock crystals were mechanically adjusted prior to take off, and later drift was recovered by geometrically matching the monostatic and bistatic image and further refine by IFSAR when aircraft separation was below critical baseline. Later ONERA/FOI experiment used GPS locked clock signals on both aircraft. This was nevertheless possible because aircraft were not too far apart and thus their GPS 4D error were highly correlated (incidentally the clock hardware was the same on both aircraft).
In order to test even more asymmetrical configuration, satellite illumination with passive receiver, we planed to use the two channel capability of our lightweight SAR system BuSARd to simultaneously receive the direct path signal from satellite for synchronisation and the signal scattered from the ground for imaging.

2 First imaging test with static receiver

Prior to conduct a flight test, we started with a static acquisition, in order to separate the clock synchronisation problem from further receiver positioning issues.

Figure 1 Ground test with the (open) aircraft pod and the two antennae for direct path (right) and scattered signal (left).

Figure 1 shows the ground installation, the radar pod was open and the two antennae position were accurately measured (there is a geodesic beacon on the spot). The location (in front of the Notre-Dame de Beauregard cathedral) offered a large scenic view to the East on the Durance valley $\sim$100 m below and the Luberon mountains in background. The antenna was pointed 10° below horizon.
A descending orbit TerraSAR spotlight image of the area was programmed, and the SAR system was programmed to continuously record the signals around the expected imaging time.

2.1 Clock signal synchronisation

Signal from the direct path was range-compressed and corrected from the known path length (between the precision satellite orbit and the direct path antenna). The peak position and phase was fitted to zero with a linear law. While

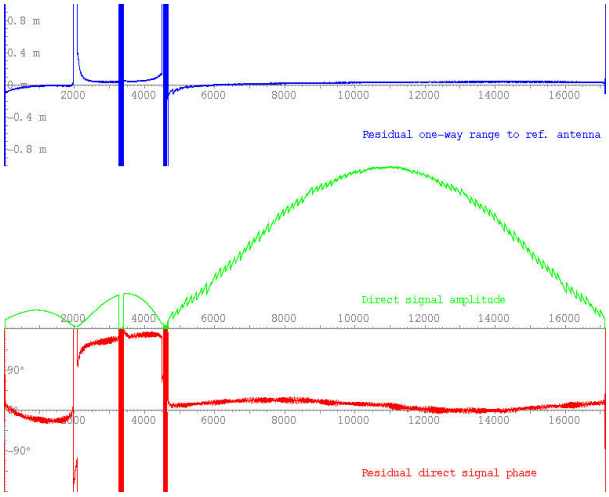

Figure 2 Ground test residual path difference (top), signal amplitude (middle) and phase (bottom) for the direct path signal.

in air-to-air bistatic acquisitions the estimation the higher order random clock fluctuations was the main technicality **[1]**, here the short 4 seconds satellite illumination does not allow clock drift rate to significantly change during integration.
One extra twist was that our sampling rate was not congruent with the transmitted pulse repeat rate, hence the induced phase slope has to be corrected for. The received signal amplitude and phase is shown on **figure 2**.
On this plot, we can observe the pre-imaging transmitter sequence with the first beam activated, visible in the first two sidelobes (with 2 transmission cuts) and then the mainlobe with the successive beam switches and eventually the final transmission cut after the last beam. We can also observe a small residual undulation (both in range and phase) that is most probably the consequence of non-modeled tropospheric delay variation while satellite elevation changes during the 4 seconds of the measure.

2.2 Static test result

The **figure 7** is the resulting bistatic SAR image.
There is no need here for autofocus beyond clock synchronisation because both receiver antennae are accurately positioned (to a few cm precision) hence the image is well registered to the ground directly from the synthesis once the initial clock offset and clock rate offset are fitted.
A ground map backdrop is added to illustrate the geometrical accuracy of the SAR image. The comparison with the monostatic TerrasarX image shows the impressive change in shadowing due to the grazing angle of the receiving antenna. Note that the monostatic image footprint is centered on the receiver location, and that the bistatic image may extend beyond the monostatic farrange because unlike in the satellite, there is no constraint in receiving signal during transmission (hence allowing continuous signal digitising and recording in our setup).

Figure 3 The BuSARd X-band radar pod used for receiving under the carrier aircraft wing (radome is open showing the antenna gimbals).

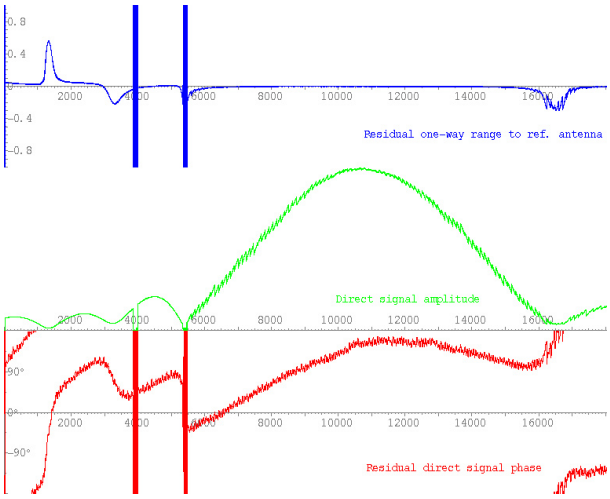

Figure 4 First (anti-parallel) flight test residual path difference (top), amplitude (middle) and phase (bottom) for the direct path signal.

3 Fight tests experiments

Two flight tests were conducted on the Salon-de-Provence area, the first one on the 2020 Nov 12th with a TerraSAR descending orbit and the second 2021 Mar 10th with an ascending orbit, both acquisitions in sliding spotlight mode centred on the ONERA building on the military air academy airbase. The first one with an anti-parallel (northbound) aircraft trajectory at 400 m ground altitude and antenna pointed 18° below horizon. The second flight was with a parallel (northbound too) aircraft trajectory at an higher altitude and antenna pointed 45° below horizon.

3.1 antiparallel flight-test result

Figure 4 show the clock synchronisation residuals for the first acquisition, showing that there is also a trajectory error induced desynchronisation.
The remaining phase slope (red curve) accounts for a minor residual mis-registration for the image but have no impact on focusing. The remaining undulation below 90°cause a minor defocus blur. Due to the extremely short acquisition time (4 s) with respect to the aircraft velocity (35 m/s) only the aircraft position bias has a significant incidence on the focusing and the geometry of the bistatic

image. In order to estimate the aircraft position update, we measured the positioning errors for a few landmarks on the image and used our SAR image geometry model to update the aircraft position bias (our standard autofocus procedure **[2]** measures mismatch between subaperture images and use the same model to update aircraft trajectory of lower and lower frequency. Thus the process used here is a sort of autofocus from image to map registration). The only difficulty was that due to the fact that the clock offset and rate biases are evaluated from direct path which itself varies with receiver position offset, and of course clock error itself induces a geometrical distortion. We could have coupled the clock and position estimates in the model, but due to the simplicity, a few geometrical model iterations were used for the estimation of the 5 modeled parameters (2 clock and 3 space biases).

Though the aircraft velocity is much lower (1/224) than the satellite velocity, and the aircraft velocity error has a negligible impact on focusing, the aircraft velocity itself is significant because of the much shorter range to target from the aircraft.

Indeed, the first (anti-parallel) acquisition raised difficulties due to the vanishing resolution at a range were angular velocities of the satellite and aircraft cancel-out. Seen from the target (the imaged ground), the bistatic acquisition measures the frequency domain distribution of the echoes on the target in the direction of the median between the transmitter direction and the receiver direction (regardless of their respective distance). Hence, for synthesizing an aperture and having a resolution in azimuth this median vector should span a sufficiently wide angle. This means that the mean angular velocities of the satellite and the aircraft seen from the ground should not cancel out (which is possible in case of anti-parallel acquisition).

Figure 8 shows first convincing result obtained by separately processing the area closer to the receiving aircraft where the angular velocity of the aircraft is dominating and the area further away where the angular velocity of the satellite dominates. The two images are then stitched together. There is, in the middle of the swath, the region where the angular velocities cancel out. In this area, the azimuth resolution is poor (not exactly vanishing to zero because the exact cancellation line varies during the acquisition) and the echoes are smeared in azimuth. This problematic area is appear as the white arc in figure 8. Incidentally, the centre for the programmed satellite sliding spotlight lies exactly at this point.

There is also a problem with the geometrical model of SAR image that fails on pixels where the angular velocities cancel at the very middle of integration. This results in a ring of misplaced radar image pixels that is more visible in the map out of the azimuth span of the SAR image. This problem requires a patch in the geometrical model which uses Newton-Raphson-like search for a point of given range and Doppler on the DTM (in fact a Armijo-damped version of it that is more numerically stable) and a brute force bracketing search as back-up in the rare cases of non-convergence. However, even this bracketing search fails across the zero-resolution line when the Doppler versus azimuth function change from increasing to decreasing. The fully bistatic-proof geometrical model should add a last-resort exhaustive search approach (grid search, particle swarm search, downhill simplex ?) for these extremely rare cases.

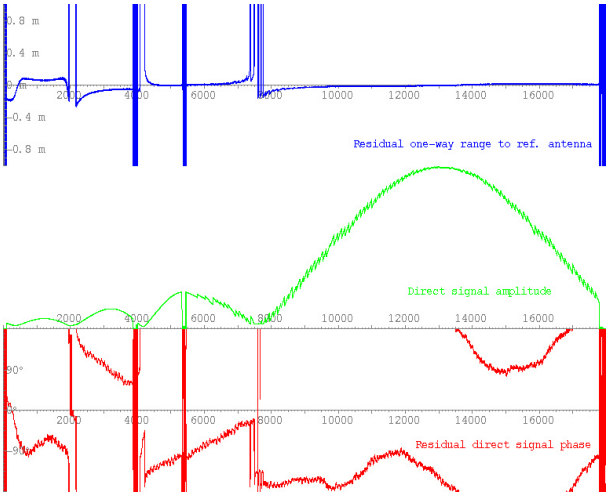

Figure 5 Second (parallel) flight test residual path difference (top), amplitude (middle) and phase (bottom) for the direct path signal. Direct path signal sliding spotlight beam steering sequence begins in the antenna second lobe because receiving aircraft was late at rendez-vous with satellite illumination.

3.2 parallel flight-test result

The second flight acquisition did not run as smoothly as the first, because the receiving aircraft was late in joining the work area and she was still climbing to the higher work altitude when the satellite began to transmit. By chance the climb leg was also northbound and the signal have been recorded.

Figure 5 show the clock synchronisation residuals for the second flight acquisition, showing that there is also a trajectory error induced desynchronisation. Furthermore unlike the former two direct channel receive, the aircraft was already in a secondary lobe of the satellite antenna pattern when the beam steering began, (she was some 3500m north of the planed latitude at acquisition). This explains why instead of having on the green curve of figure 5 an enlarged mainlobe (each beam switching makes a saw tooth that partially “winds back” along the true antenna mainlobe) we have a saw-tooth secondary lobe (on the graph, the signal used for image synthesis starts some 100 pulses after the second cut) then a null and the incomplete mainlobe.

In longitude also, the receiver position was not as planed, instead of being looking towards the ONERA building from a position some 2 km West of it, the sensor was 2.5 km East of the target. Hence our target setup was on the wrong side of the flight track, out of the receiving antenna mainlobe.

The **figure 9** shows the resulting image for the second (parallel) flight projected to the ground using the level 2 DTM used for focusing. Though there is not the problematic azimuth unresolved area with parallel tracks, the image is less appealing than the previous one due to both the steeper an-

tenna pointing (45° below horizon) and an higher area in the middle of the image that shadows terrain further away from the receiver. Marginally, the centre of the illuminating beam is some 5 km behind meaning that the area further away is also less illuminated from the satellite.

4 future work

Work on these first two acquisitions is still in progress, with two issues: The satellite antenna pattern compensation requires estimation of the beam scanning sequence (the antenna pattern itself is well documented in the TerraSAR-X image metadata but not the precise antenna seering sequence, hence only receiving antenna pattern is compensated for in figures 7 to 9). The noise spectrum power density is well estimated from scattered signal (as recording is continuous we selected an area away from the scattered echoes) however, the eventual image noise level depends on the antenna pattern compensation. Once both transmit and receive antennae pattern are compensated, we plan to use the relative noise level to delineate the useful bistatic image area.
During the 2009 experiment, the lightweight system itself was (monostatically) imaged in flight when it crossed the illumination beam **[3]**. In the satellite illumination case, the same receiving aircraft was in the imaged swath from the TerraSAR satellite. Even if we do not have access to the satellite raw data (unlike that of our own heavy SAR system RAMSES in 2009) it is theoretically (and practically see my other presentation) possible to post-process the complex valued single look satellite image to refocus it on our aircraft instead of the landscape. First attempts are not very conclusive, but it is probably due to the low RCS of our aircraft (she is a composite touring motor glider). Her 2009 radar image **figure 6** shows that the brighter contribution to RCS is the X-band radar antenna in the pod. This image is on a dark background because the target velocity was more significant (about 25of the imager velocity as radial component) and the target was almost "off clutter" in this experiment. During further acquisitions, we will take opportunity to have the receiver aircraft fly on a track such as it will appear above a dark water surface on the monostatic satellite image, thus making it possible to see more details of her than just a couple of point echos such as the X-band direct path antenna reflection.
As we have a sequence of satellite acquisition programmed for a biomass studies at ONERA, we hope to use these acquisitions for further bistatic experiments, first with perpendicular track configurations with front looking receiver aircraft in horizontal flight, and later with front looking aircraft in steepest possible descent rate towards imaged area. The idea is to prepare an opportunity of testing bistatic imaging of the landing area with the receiver on a probe rocket during reentry in order to demonstrate the possible use of bistatic SAR for targeting hypersonic reentering vehicle to an aircraft carrier at sea (unlike for landing on ground runway, navigation to a vessel at sea cannot resort to sideways imaging of landmarks whose position relative to the runway is accurately known and only bistatic SAR allows imaging in the exact direction the sensor is heading at).

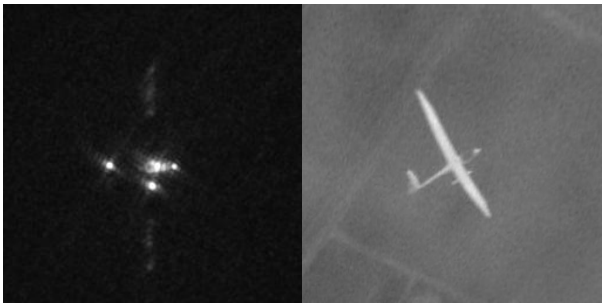

Figure 6 Air-to-air ISAR monostatic image acquired in 2009 of the receiving aircraft during an acquisition from our late heavy SAR system RAMSES (left). In flight photo of the receiving aircraft from the imaging aircraft for comparison (right). The brighter spot under the wing is the X-band receiving antenna visible through the radome, bright spot at the rear is a specular reflection at the rudder/fuselage junction.

5 Acknowledgements

Air academy airbase ATC and the test-pilot involvement in operating an aircraft only certified for daytime flight for acquiring signal from a dusk/dawn polar orbiting satellite should be emphasized.
The area map used for image backdrop are provided by the Institut Géographique National under the public open data initiative.

6 Literature

[1] Cantalloube,H.; Wendler,M.; Giroux,V.; Dubois-Fernandez,P.; Horn,R.: A first bistatic airborne sar interferometry experiment - Preliminary results, Sensor Array and Multichannel Signal Processing Workshop, 2004, pp.667-671

[2] Cantalloube,H. M. J.; Nahum,C. E.: Multiscale local map-drift-driven multilateration SAR autofocus using fast polar format image synthesis, IEEE Transactions on Geoscience and Remote Sensing, vol 49-10 part 1, 2011, pp.3730-3736

[3] Cantalloube, Hubert M. J.; Nahum, Carole E.: An opportunity Air-to-Air Inverse SAR imaging experiment: Autofocus and Image Synthesis issues, 8th European Conference on Synthetic Aperture Radar, 2010, pp.1-4

Figure 7 Bistatic image from the ground test overlaid on a terrain map (top). Map of the area for reference (middle). Corresponding monostatic TerrasarX image (bottom). Note that monostatic image is Hamming-weighted, unlike the bistatic one.

Figure 8 Bistatic image with airborne receiver flight anti-parallel to transmitting satellite track (top). Map of the area for reference (middle). Corresponding TerraSAR-X monostatic image (bottom). White smeared area correspond to where the satellite and aircraft angular velocities are exactly opposite.

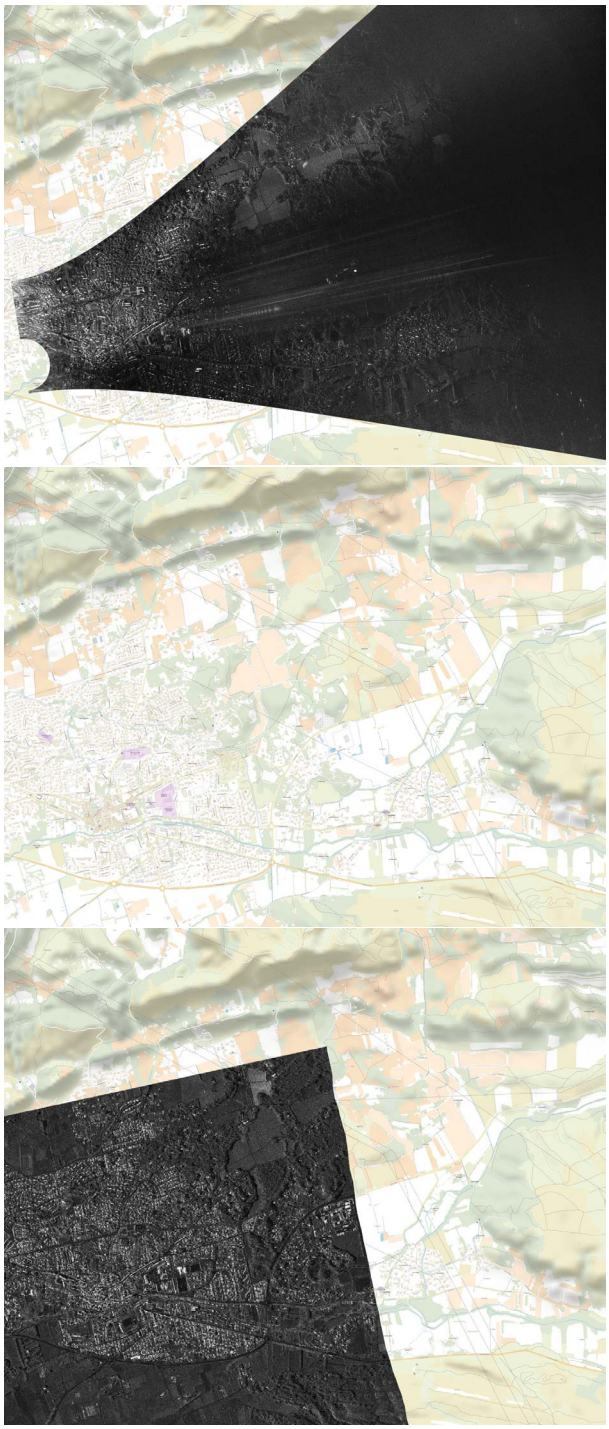

Figure 9 Bistatic image with airborne receiver flight parallel to transmitting satellite track (top). Map of the area for reference (middle). Corresponding TerraSAR-X monostatic image (bottom). Monostatic image centre is at the South-West corner because aircraft was late at rendez-vous hence not pointed towards the scene centre.

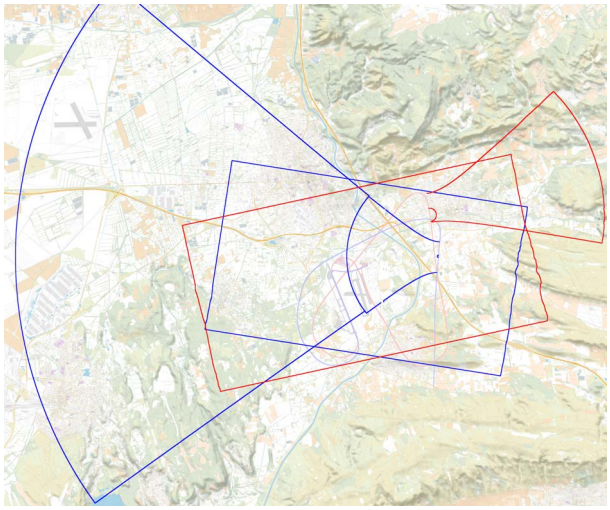

Figure 10 Footprints of the monostatic and bistatic images for the first anti-parallel test-flight (dark blue) and for the second parallel test-flight (red). Aircraft trajectories are plotted in light blue and pink respectively.
It shows that the aircraft was correctly aligned with satellite illuminated area for the first (blue) test-flight.
But for the second (red) flight-test, the aircraft was off the spotlight axis -hence the side-lobe illumination at the beginning of the acquisition- and looking away from the satellite illumination maximum.
That and the steeper receiving antenna pointing severely reduces the bistatic image useful range.